

Preliminary Experimental Measurements of the Dielectric and Magnetic Properties of a Material with a Coaxial TDR Probe in Reflection Mode

Iman Farhat^{1, *}, Lourdes Farrugia¹, Raffaele Persico^{2, 3},
Sebastiano D'Amico⁴, and Charles Sammut¹

Abstract—This paper presents a technique based on time domain reflectometry (TDR) to determine the dielectric and magnetic properties of lossless materials fitted inside a transmission line section. The proposed method involves three different line terminations namely open, short, and matched load. The described technique involves placing a sample of material under test (MUT) inside a terminated transmission line and exciting this with a vector network analyser from the other end to measure the reflection coefficient. Results achieved from a transmission line model were compared with numerical simulations obtained using CST Microwave Studio. The comparison shows that the electric and magnetic properties of a material may be determined precisely with this technique. Experimental results are also presented to validate the proposed method. Estimates of measurement errors, resulting from sample length uncertainty, vector network analyser uncertainty, and open-end inaccuracy are discussed.

1. INTRODUCTION

Measurements of dielectric and magnetic properties of materials have been historically associated with the design of suitable devices. In particular, the application of time domain reflectometry (TDR) in engineering and natural science has been of interest since the 1930s, when it became a recognized technique for cable testing [1]. This testing method relies on the change of impedance along the transmission line, which generates a partial or total reflection of the travelling waves. In particular, the spatial location of a defect in the cable can be determined by measuring the time between the launch of the wave into the cable and the detection of reflections using the known propagation velocity of the waves on the transmission line. Later on, the method was modified using the spatial location of the reflection point to calculate the propagation velocity of the waves inside a MUT that filled up a piece of cable or a piece of waveguide [1]. In 1969, Fellner-Feldegg [2] was the first to report the use of TDR for measuring the dielectric constant of liquids. Davis and van Chudobiak (1986) introduced the TDR techniques in the field of soil water content measurement [3].

The main aim of this study is to investigate the determination of the dielectric permittivity and magnetic permeability of a MUT for a wide range of applications using TDR. The method is based on the classical Nicholson-Ross method [4] and is an extension to the technique reported in [4]. In particular, with respect to [4], here not only simulated data but also experimental data are considered.

Since a material's molecular structure defines its dielectric properties, if the molecular structure changes, so will the dielectric properties. Thus, in general, the TDR probe can indirectly measure other properties that are also correlated to the molecular structure and can be a valuable alternative when the property of interest is difficult to measure directly [5].

Received 19 November 2019, Accepted 10 March 2020, Scheduled 14 April 2020

* Corresponding author: Iman Farhat (iman.farhat@um.edu.mt).

¹ Department of Physics, University of Malta, Malta. ² Institute for Archaeological and Monumental Heritage IBAM-CNR, Italy.

³ International Telematic University Uninettuno, UTIU, Italy. ⁴ Department of Geoscience, University of Malta, Malta.

Time domain reflectometry (TDR) is not only one of the less expensive and more accurate tools for dielectric properties determination of materials and water soil content but also a useful technique in order to provide users with an on-site measurement option. Thus, it can provide advantage over various methods to measure soil volumetric water content and dielectric and/or magnetic properties. Unlike the common gravimetric method, TDR in situ measurements enable continuous and non-destructive monitoring of moisture content in soils, rocks, and building materials [6]. They can also be utilized to detect water condensation processes in building envelopes during wintertime and can offer an assessment tool for design solutions that can be adopted by civil engineers [1]. Furthermore, the measurement of material electromagnetic properties in the agriculture and food processing industry has been of interest for many years. For instance, the knowledge of dielectric properties of foods as a function of moisture content is essential in the design and control of drying systems [7]. Moreover, FDR is widely used in biomedical applications for diagnostic and monitoring purposes [8].

In this paper, we propose an inversion algorithm based on the least square difference between model data based on the theory of the transmission lines and the measured data [9]. This will require one more step with respect to the use of simulated data. In particular, it is needed to calculate the reflection coefficient at the reference plane, which is not the same as the plane at which it is measured, because of the unavoidable presence of connections between the piece of with the MUT inside and the rest of the coaxial structure. The advantage of this technique concerning the classical method of Nicholson and Ross is that that the method is based on waveguide measurements. Furthermore, it implies that the system is usually not portable in the field (e.g., for geophysical measurements), but rather samples of MUT have to be collected from the field and brought to the laboratory taking care not to alter their properties of compactness, moisture content, and original temperature. Moreover, for frequencies below 1 GHz, the needed cross-section of a waveguide increases and becomes progressively more critical. Finally, even if (as hypothesized in the paper) the MUT is dispersionless, the waveguide presents some modal dispersion that the transmission line based on the TEM mode does not show.

The paper is organized as follows. The formulation of the problem is described in Section 2. Section 3 illustrates the procedures followed to obtain either simulated and experimental data which are then compared in Section 4. Section 5 provides details of the inversion procedure and the achieved inversion results, leading on to the conclusion.

2. FORMULATION OF THE PROBLEM

This section presents the derivation of the three cases that allow computing the permittivity and permeability of a MUT from the measured reflection coefficient at the chosen reference plane of a coaxial transmission line. Besides this, the section defines a novel algorithm approach to retrieve the dielectric permittivity and magnetic permeability of a material from an inverse problem approach.

2.1. Theoretical Framework

The most well-known methods to determine the permittivity and permeability of a sample of material are the Nicolson-Ross-Weir (NRW) [4] and the Baker-Jarvis (BJ) iterative methods [10]. Both methods are based on the measurement of the reflection and transmission coefficients in a transmission line or a waveguide embedded in or filled up with the MUT. However, this paper proposes an approach for a lossless transmission line partially filled with (or partially embedded in) a possibly lossy MUT, related to its reflection coefficient for three different types of termination [11, 12]. This goal has been achieved by gathering data with a coaxial cable, part of which is filled up with the same MUT and making use of three different terminations, namely a short-circuited transmission line, an open transmission line, and a transmission line terminated with a matched load (to be understood as a load matched to the previous section line in absence of the MUT). The reflection coefficient is calculated at the reference plane placed just before the MUT, starting from the physical accessible input measurement plane.

Figure 1 shows the schematic of the three terminations with the MUT filling a coaxial line section of length L whose complex permittivity, complex permeability, and characteristic impedance are denoted as ϵ_r , μ_r , and Z_{l_2} , respectively. The datum is the reflection coefficient (S_{11}) at reference planes $x = -L$, the termination at $x = 0$. Within the region $-L \leq x \leq 0$, which is filled with the MUT, the characteristic

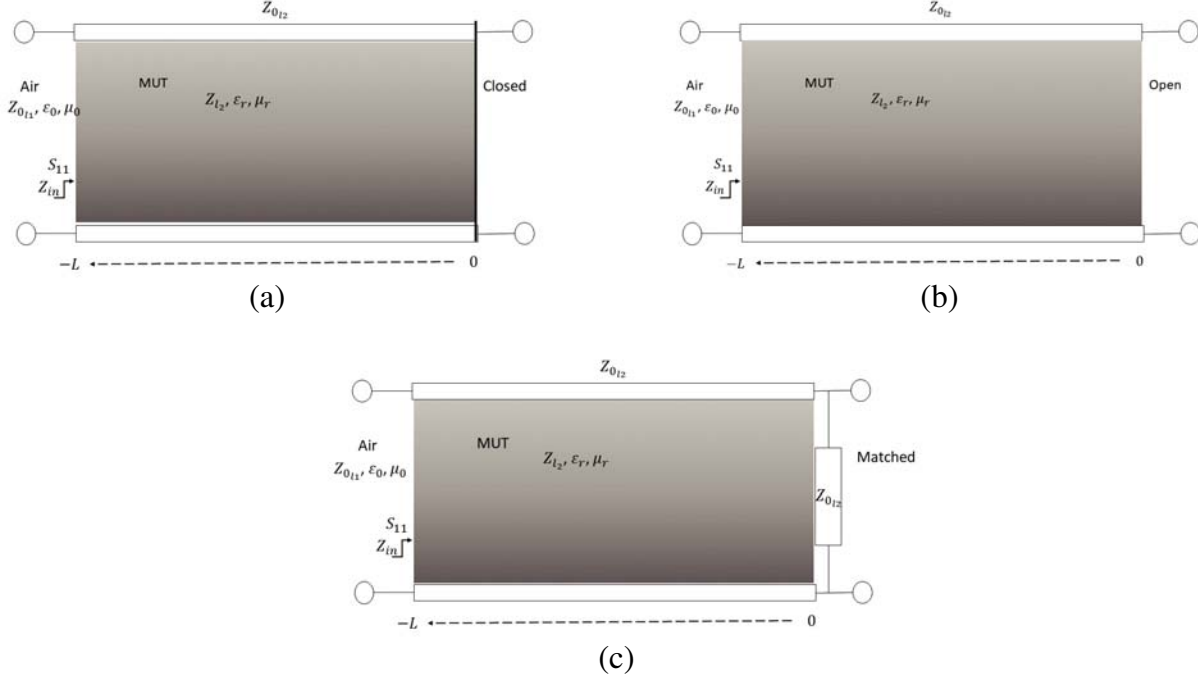


Figure 1. Schematic of the S_{11} -parameter and the input impedance of the sample-loaded transmission line. (a) Short-circuited line. (b) Open-circuited line. (c) Matched-circuited line.

impedance is $Z_{l_2} = \sqrt{\frac{\mu_r}{\epsilon_r}} Z_{0_{l_2}}$, where μ_r and/or ϵ_r are complex if the medium is lossy and are real if the medium is lossless. The reflection coefficient of a wave incident at $x = -L$ (referred to as datum) from the air-filled line is given by

$$\Gamma = \frac{Z_{-L} - Z_{0_{l_1}}}{Z_{-L} + Z_{0_{l_1}}} \quad (1)$$

where $Z_{0_{l_1}}$ is the characteristic impedance of the air-filled transmission line before part which is filled with the MUT, and Z_{-L} is the impedance of the termination at $x = 0$ transformed to the reference plane at $x = -L$. Thus, for the short-circuited transmission line the input impedance is given by

$$Z_{-L} = jZ_{0_{l_2}} \frac{\mu_r}{\epsilon_r} \tan(k_0 \sqrt{\mu_r \epsilon_r} L) \dagger \quad (2)$$

where k_0 is the wave number in free space. For the transmission line terminated with an open circuit, the input impedance at $x = -L$ is

$$Z_{-L} = -jZ_{0_{l_2}} \frac{\mu_r}{\epsilon_r} \cot(k_0 \sqrt{\mu_r \epsilon_r} L) \quad (3)$$

Finally, the impedance at $x = -L$ of the transmission line terminated with a matched load is

$$Z_{-L} = \sqrt{\frac{\mu_r}{\epsilon_r}} Z_{0_{l_2}} \frac{1 + j \sqrt{\frac{\mu_r}{\epsilon_r}} \tan(k_0 \sqrt{\mu_r \epsilon_r} L)}{\sqrt{\frac{\mu_r}{\epsilon_r}} + \tan(k_0 \sqrt{\mu_r \epsilon_r} L)} \quad (4)$$

Provided that the MUT fills the transmission line section up to $x = -L$, the reflection coefficient at this reference plane when the line is terminated with a short circuit can be reformulated using Eqs. (1)

[†] Though TDR stands for the time domain, the approach is conducted in the frequency domain.

and (2):

$$\Gamma_{\text{short}}(-L) = \frac{\left(Z_{0l2} \sqrt{\frac{\mu_r}{\varepsilon_r}} - Z_{0l1} \right) + e^{-2j \frac{2\pi f L}{c_0} \sqrt{\mu_r \varepsilon_r}} \left(Z_{0l2} \sqrt{\frac{\mu_r}{\varepsilon_r}} + Z_{0l1} \right)}{\left(Z_{0l2} \sqrt{\frac{\mu_r}{\varepsilon_r}} + Z_{0l1} \right) - e^{-2j \frac{2\pi f L}{c_0} \sqrt{\mu_r \varepsilon_r}} \left(Z_{0l2} \sqrt{\frac{\mu_r}{\varepsilon_r}} - Z_{0l1} \right)} \quad (5)$$

Similarly, for the reflection coefficient when the transmission line is terminated with an open circuit, Equation (6) can be obtained by substituting from Equation (3) into Equation (1).

$$\Gamma_{\text{open}}(-L) = \frac{\left(Z_{0l2} \sqrt{\frac{\mu_r}{\varepsilon_r}} - Z_{0l1} \right) - e^{-2j \frac{2\pi f L}{c_0} \sqrt{\mu_r \varepsilon_r}} \left(Z_{0l2} \sqrt{\frac{\mu_r}{\varepsilon_r}} + Z_{0l1} \right)}{\left(Z_{0l2} \sqrt{\frac{\mu_r}{\varepsilon_r}} + Z_{0l1} \right) - e^{-2j \frac{2\pi f L}{c_0} \sqrt{\mu_r \varepsilon_r}} \left(Z_{0l2} \sqrt{\frac{\mu_r}{\varepsilon_r}} - Z_{0l1} \right)} \quad (6)$$

The reflection coefficient with the transmission line terminated by a matched load is obtained by substituting Eq. (4) in Eq. (1) giving:

$$\Gamma_{\text{load}}(-L) = \frac{\left(\sqrt{\frac{\mu_r}{\varepsilon_r}} + 1 \right) \left(Z_{0l2} \sqrt{\frac{\mu_r}{\varepsilon_r}} - Z_{0l1} \right) - \left(Z_{0l2} \sqrt{\frac{\mu_r}{\varepsilon_r}} + Z_{0l1} \right) e^{-2ja}}{\left(\sqrt{\frac{\mu_r}{\varepsilon_r}} + 1 \right) \left(Z_{0l2} \sqrt{\frac{\mu_r}{\varepsilon_r}} + Z_{0l1} \right) - \left(Z_{0l2} \sqrt{\frac{\mu_r}{\varepsilon_r}} - Z_{0l1} \right) e^{-2ja}} \quad (7)$$

where $a = k_0 \sqrt{\mu_r \varepsilon_r} L = \frac{2\pi f}{c_0} \sqrt{\mu_r \varepsilon_r} L$, Z_{0l2} is the characteristic impedance of the transmission line before inserting the MUT. Z_{0l1} is the intrinsic impedance of the transmission line in the part preceding the MUT.

The numerical value for ε_0 is about 8.854×10^{-12} F/m and for μ_0 is 1.26×10^{-6} H/m. In propagation media different from the free space, the permittivity and permeability are usually expressed respectively as the products $\varepsilon_r \varepsilon_0$ and $\mu_r \mu_0$, where ε_r and μ_r represent the dimensionless relative permittivity and relative permeability, respectively. In lossy isotropic media, ε_r is complex and can be expressed as

$$\varepsilon_r = \varepsilon' - j\varepsilon'' \quad (8)$$

where ε' and ε'' are both positive and in general depend on frequency. Similarly, μ_r is complex in media with magnetic losses, so that it can be expressed as

$$\mu_r = \mu' - j\mu'' \quad (9)$$

where μ' and imaginary part μ'' are both positive and in general depend on the frequency.

3. SIMULATED AND EXPERIMENTAL DATA

In this section, the problem is formulated by assuming that the TDR probe consists of a section of coaxial transmission line shorted at one end and filled with a homogeneous MUT. To validate the proposed method, the coaxial section was simulated using CST Microwave Studio. This section presents the measurements setup and procedure using a coaxial sample holder to determine the reflection coefficient of the MUT. We then describe the optimisation algorithm used to achieve convergence to the global minimum of the cost function, in order to retrieve the dielectric permittivity and permeability profile of the MUT from the measured reflection coefficient.

3.1. Simulated Data

In order to validate the proposed inversion analysis, a coaxial air-filled line of 40 cm long and terminated by a short circuit was modelled with the CST full-wave simulator to obtain the reflection coefficient (see Figure 2). A lossless non-dispersive magnetic material was then considered whose relative permittivity and permeability were chosen as $\varepsilon_r = 5$ and $\mu = 2$. The dimensions of the inner and outer radii of the coaxial line were designed to satisfy an input impedance at $x < -L$ of 50Ω impedance of the VNA test port. The intrinsic impedance of the coaxial section intended to host the MUT, when void, is 50Ω .



Figure 2. CST coaxial line model.

The internal diameter of the coaxial section was 3 mm, and the diameter of the center conductor was 1.25 mm. The coaxial line was excited at the input reference plane ($x = -L$) and simulated over a frequency range from 500 MHz to 1 GHz, in 21 MHz steps, using the CST Studio suite time-domain solver. From simulation results, the reflection coefficient at the reference plane was extracted and imported to an in-house MATLAB code to retrieve the required properties of the MUT.

3.2. Uncertainties

For accurate estimation of the measurement method, two primary error sources, i.e., the sample length error and the finite accuracy of reflection coefficient measurement, are considered. In the experiment, no direct measurement is possible at the measurement plane of interest. Therefore, the calibration was conducted at a calibration plane, at the end of the coaxial transmission line (see Figure 4). Then, at the sampled data post-processing stage, a phase correction was applied to shift the calibration plane to the measurement plane. The measured reflection coefficient can be calculated as follows [13],

$$\Gamma_{\text{measured}} = S_{e11}\Gamma_{\text{correct}} \quad (10)$$

where Γ_{correct} is the corrected reflection coefficient, and S_{e11} is an error parameter that can be determined from calibration. To find the error coefficient three independent measurements should be sampling three different reflection standards. For this purpose, open, short, and load were used with reflection coefficients Γ_o^{cal} , Γ_s^{cal} , and Γ_{lo}^{cal} . Then the error coefficient can be expressed in terms of calibration standards as follows:

$$D = \frac{2(\Gamma_o^{\text{cal}} - \Gamma_{lo}^{\text{cal}})}{\Gamma_o^{\text{cal}} - \Gamma_s^{\text{cal}}} \quad (11)$$

$$D = \frac{1 + E - D}{DE - E - 1} \quad (12)$$

$$C = \frac{(\Gamma_o^{\text{cal}} - \Gamma_s^{\text{cal}})(1 - B)}{2} \quad (13)$$

$$A = \Gamma_o^{\text{cal}} - \frac{C}{1 - B} \quad (14)$$

where $A = S_{e11}$, $B = S_{e22}$, $C = S_{e21}^2$, $E = e^{-j2\beta l_1}$, and l_1 is the offset length. Furthermore, in order to retrieve the dielectric properties from S_{11} parameters, the reference plane needs to be changed from the calibration plane to the measurement plane multiplying Γ_{correct} by $e^{-j2\beta l}$.

3.3. Experimental Data

The measurement setup consists of a vector network analyzer (Rohde & Schwarz, ZVA 50, 10 MHz–50 GHz) in combination with an open-ended transmission line. The operational frequency of the measurements to measure the dielectric properties is in the range from 500 MHz to 1 GHz. The coaxial transmission line sample holder is shown in Figure 3, where the MUT is loaded inside the line. The transmission line is a commercial available coaxial adapter 50 (SPINNER GmbH, Munich, Germany) used in RF-applications. It is configured such that it allows phase flow through the sample. In order to connect the two-Port Coaxial Transmission Line with the vector analyser from one-end and short it from the other end, two SMA adapters are used. However, the connectors used to terminate the transmission line and to connect to the vector network analyser (VNA) introduce a phase delay. This



Figure 3. Measurement set-up.

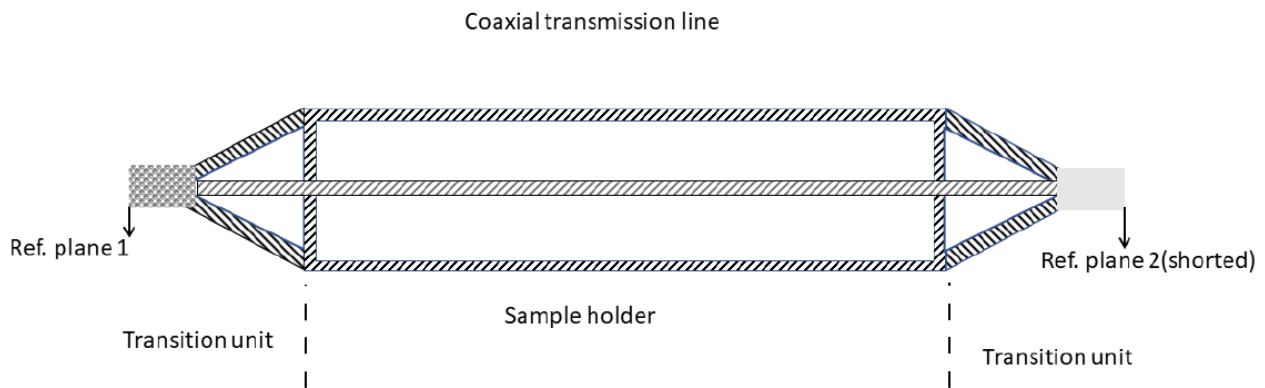


Figure 4. Schematic of the coaxial sample holder used in measurements.

presents a technical challenge since the theoretical considerations take into account the MUT fitting exactly in the sample holder, between the termination and the reference plane. The MUT is loaded into the sample holder, and all parts are tightly screwed together. The length of the coaxial section is 11.2 cm with internal diameter of 6.85 mm and a center conductor diameter of 3 mm. Consequently, the characteristic impedance without the MUT is 49.5Ω , which enables only the TEM mode to propagate along the line in the frequency range of interest. For the inversion, the data with the transmission line terminated by a short are considered.

Before the dielectric measurements, a one-port calibration was performed in order to compensate the influences of the cable connecting the sample holder to the VNA, using a mechanical calibration kit (Agilent 85032F). For a one-port calibration, reflection measurements for an open, a matched load, and a short circuit termination were required. However, the measured signals at the VNA test port contain information not only from the sample under test but also from the sample cell and its adapter. In Figure 4, the reference plane 1 is the actual VNA measurement port. Therefore, the VNA input signal is transformed to the MUT plane through the transition region. There is a reflection at this point, but the signal proceeds to the other end of the MUT coaxial section, where there is another reflection at the second transition. The signal then proceeds through the second transition region, at the end of which there is another reflection, depending on the type of termination. The second signal then has to traverse back through the second transition, through the MUT and the first transition until it reaches the VNA test port. The analysis has to account for all these, neglecting additional reflections.

Two test samples were chosen for a preliminary validation experiment, namely air and Teflon. These materials are non-dispersive and possess low loss properties which serve to validate the ability of the proposed inversion method to retrieve permittivity and permeability profiles for lossless or low-loss materials from the measured reflection coefficient (S_{11}). Once the S_{11} -parameter of the sample holder had been obtained, the data were processed to remove the phase delay caused mentioned previously.

After the contribution of unwanted connectors sections was removed, the permittivity and permeability of the test samples could be determined by using the direct inversion algorithm. For the purpose of comparison, the coaxial sample holder was modelled in CST, and simulation and measurement results were compared with the transmission line mathematical model. Figure 4 illustrates the schematic configuration of the coaxial sample holder used in this experiment.

4. COMPARISON BETWEEN SIMULATED AND EXPERIMENTAL CALIBRATED DATA

Before showing a comparison between simulated (full wave) and experimental data, in Figure 5 we present a comparison between CST simulated data and data calculated from transmission line theory. In this way, we obtain a preliminary evaluation of the presumable reliability of the method (and of the correctness of the implemented codes), without considering the added complication of moving the reference plane. For this first comparison, we chose an idealized lossless medium with $\epsilon_r = 5$ and $\mu_r = 2$, terminated with short. The parameters of the cable and the frequency range are those provided in Section 3.1. In particular, Figure 5 represents the real (a) and imaginary (b) parts of the simulated reflection coefficient as functions of frequency and the data obtained by the transmission line model of Equation (5). The agreement between the transmission line data and the data obtained from the full wave simulation is very good. Because the MUT is lossless, the real and imaginary parts of the reflection coefficient fluctuate between ± 1 over the frequencies of interest.

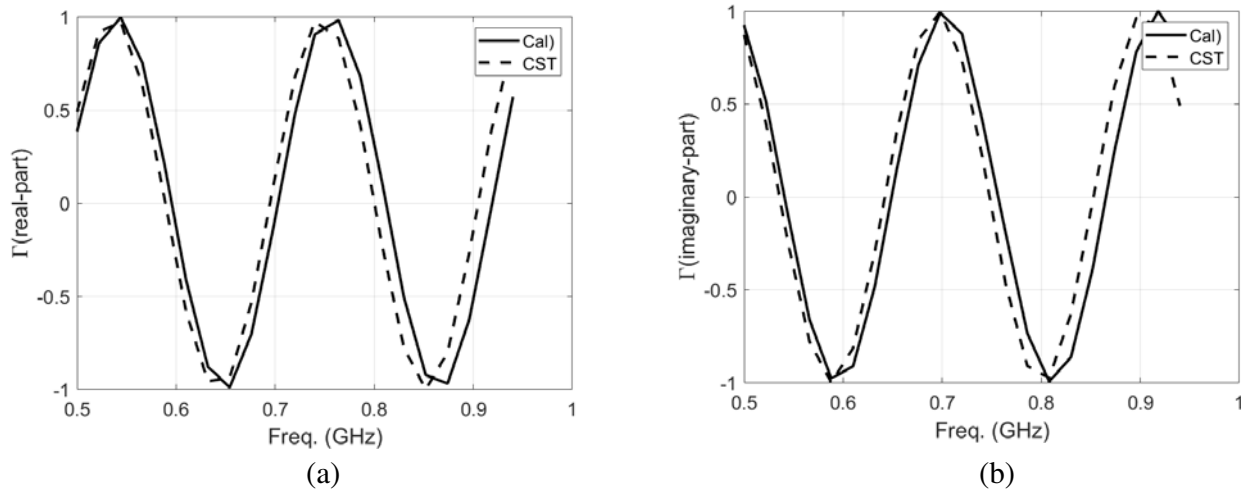


Figure 5. The solid lines indicate the reflection coefficient calculated from theoretical consideration of a short-circuit terminated transmission line section, and the dashed lines represent the CST simulated results. (a) The real part of the reflection coefficient. (b) The imaginary part of the reflection coefficient.

In order to make an initial comparison between CST and calibrated experimental data, an empty coaxial section was considered. The results shown in Figure 6 represent the real (a) and imaginary (b) parts of the reflection coefficient as a function of the frequency measured by the VNA on the coaxial sample holder together with the simulated data obtained with a CST model. The experimental data in Figure 6 involve phase delay arising from the input connector. There is substantial similarity between the two data sets, but the discrepancy increases with frequency. In Figure 7, the phase delay was corrected showing the reflection coefficient compared with that simulated by the CST software. The agreement is visibly better, thus validating the correctness of the calibration procedure.

A second validation experiment was performed using Teflon as MUT. The nominal value of the relative dielectric permittivity of the available Teflon insert was $\epsilon_r = 2$. Teflon shows negligible losses and negligible relative permeability. Figure 8 shows the real (a) and imaginary (b) parts of the measured and simulated reflection coefficients (without phase correction) as a function of frequency. Figure 9 shows

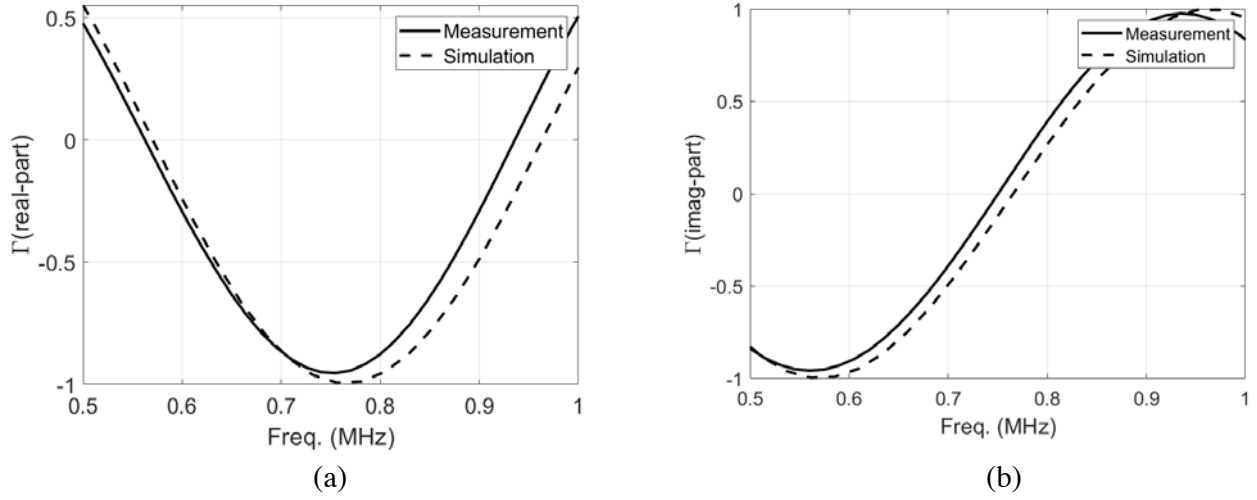


Figure 6. The reflection coefficient (real and imaginary parts) of the air as the MUT simulated at port 1, no phase correction was implemented on the measured reflection coefficient. (a) Real part of the reflection coefficient. (b) Imaginary part of the reflection coefficient.

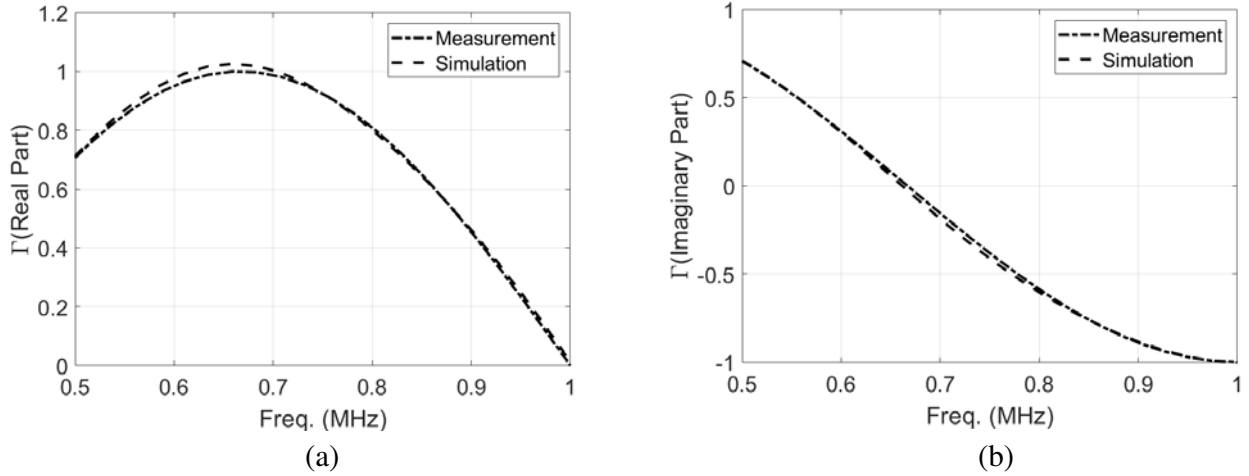


Figure 7. The reflection coefficient (real and imaginary parts) of air as the MUT after phase correction. (a) Real part of the reflection coefficient. (b) Imaginary part of the reflection coefficient.

the same comparison after phase correction of the experimental data, which reconfirms the validity of the phase correction using Eq. (10). The slight difference between corrected experimental data and simulation results may be because the Teflon insert did not fit tightly in the coaxial line test section.

4.1. Inversion Details and Result

Our inversion algorithm implements a least square minimization of the cost function of Equation (5), involving the measured and modelled reflection coefficients and considering the two auxiliary unknowns $\alpha = \sqrt{\frac{\mu_r}{\epsilon_r}}$ and $\beta = \sqrt{\epsilon_r \mu_r}$. For lossless cases α and β and consequently ϵ_r and μ_r are real. However, our inversion algorithm is conceived for complex quantities, and it does not assume *a-priori* that the MUT is lossless.

The minimization was exhaustive and was performed on 101 cells for each of the four unknowns searched for (namely the real and imaginary parts of α and β). This amounts to a total of $101^4 =$

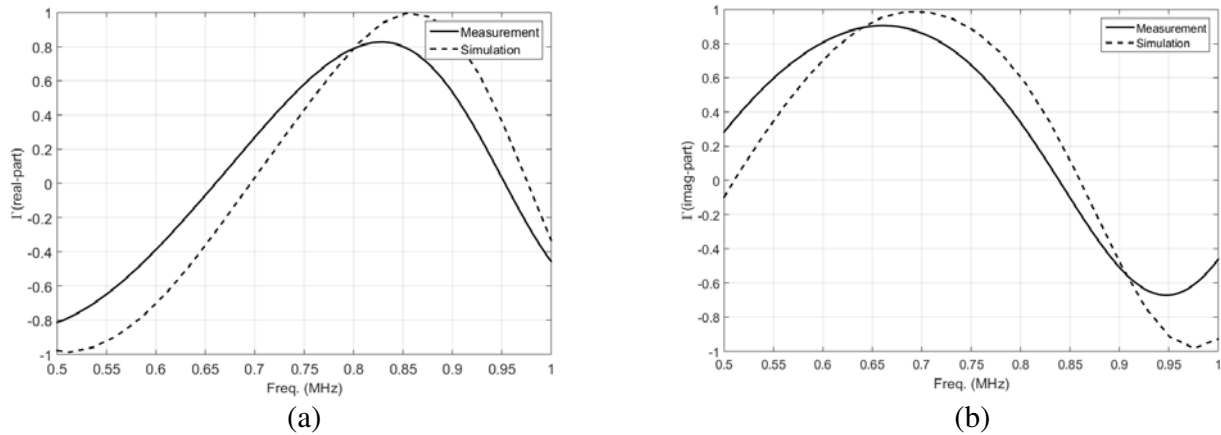


Figure 8. The reflection coefficient (real and imaginary parts) at the reference plane of the coaxial test section containing Teflon as the MUT without phase correction. (a) Real part of the reflection coefficient. (b) Imaginary part of the reflection coefficient.

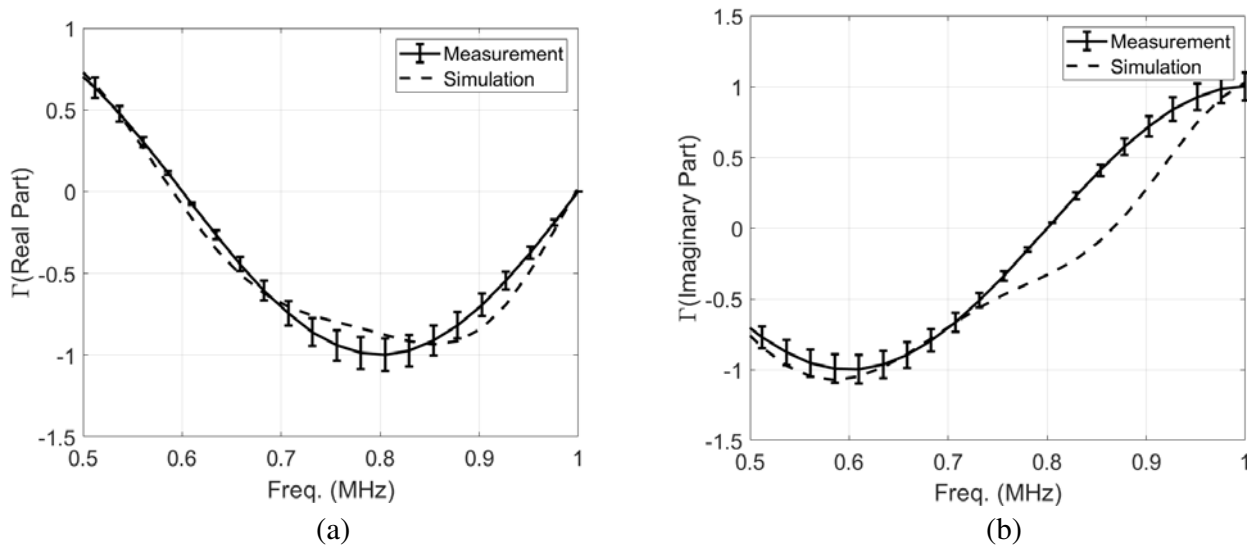


Figure 9. The phase-corrected reflection coefficient (real and imaginary parts) at the reference plane of the coaxial test section containing (Teflon as the MUT). (a) Real part of the reflection coefficient. (b) Imaginary part of the reflection coefficient.

104060401 values to be compared. We consider a hyper-rectangle in R^4 such that $\text{Re}\{\alpha_r\} \in [0.01 : 3.995]$, $\text{Im}\{\alpha_r\} \in [-2 : 2]$, $\text{Re}\{\beta_r\} \in [1 : 21]$, and $\text{Im}\{\beta_r\} \in [-4 : 0]$. This hyper rectangle directly imposes the physically modelled conditions $\text{Re}\{\alpha_r\} > 0$, $\text{Re}\{\beta_r\} \geq 1$, $\text{Im}\{\beta_r\} \leq 0$.

The minimization procedure is implemented with a nested-loop iterative algorithm such that its n th iteration exhaustively minimizes the cost function in a hyper-rectangle centred on the values from the previous iteration and reduced in size with respect to the previous step. This reduces the size of the pixels in the 4-dimensional space wherein the solution is searched for, and therefore it allows better approach the global minimum of the cost function.

The optimization procedure is designed to stop when both ϵ_r and μ_r at the $(n - 1)$ th step and at the n th step differ by less than 2% or alternatively when the minimum value of the cost function at the n th step is larger than the homologous value found at the $(n - 1)$ th step. The minimization

is implemented by means of an in-house MATLAB code, which reads as inputs of the parameters of the cable, frequency range, frequency step, and data, that in turn can be read from an external file containing either the result of a CST simulation or the measured and phased-corrected experimental data.

In the case of the simulated medium with $\varepsilon_r = 5$ and $\mu_r = 2$, the solution of the inverse problem resulted in $\varepsilon_r = 4.7297 - 0.7789i$ and $\mu_r = 1.9849 + 0.3269i$. The inversion algorithm converged after 20 iterations, each of which required about 10 minutes on a laptop computer with 16 Gb RAM. This resulted in an error of 0.04% in estimating the relative permittivity and 0.58% in estimating the relative permeability. Though the algorithm converged to the modelled parameters accurately, false imaginary parts were induced. This is possible because the algorithm searches for complex quantities. In particular, there is a non-physical value of the imaginary part of the magnetic permeability, which is also possible because the physical conditions to respect have been imposed on the auxiliary unknowns α and β and not directly on the unknowns of interest ε_r and μ_r .

With regards to experimental data, in the case of the MUT being air, the minimization of the cost function provided $\varepsilon_r = 0.9022$ and a relative permeability of $\mu_r = 1.1084$. In this case, the inversion algorithm converged after 50 iterations. This resulted in an error of 0.098% estimating relative permittivity and 0.108% with respect to the relative permeability. In the case of Teflon as the MUT, we achieved as result of the minimization of the cost function $\varepsilon_r = 1.9100 - 0.0525i$ and $\mu_r = 1.0313 + 0.0284i$. The error with respect to the nominal value of the properties of the material is (considering the complex achieved result) 0.04% with respect to the relative permittivity and 0.03% with respect to the relative permeability.

5. CONCLUSION

A novel technique to measure both the dielectric and magnetic properties of a material using a TDR probe modelled as a coaxial line section, terminated with a short circuit at one end was presented. Furthermore, terminations with open or matched load are mathematically modelled. The originality of the inversion method consists in the fact that the data are gathered only in reflection mode and that the extracted data included the relative permeability which previously could only be obtained by using a two-port measurement technique, considering both reflection and transmission coefficients. This also constitutes a preliminary step toward applications where reliable data in transmission mode are difficult to achieve. The model was validated both with respect to full wave numerical data simulated with CST and experimental data obtained with a commercial coaxial line section. For the experimental data, however, a phase correction was required in order to extend the reference plane up to the MUT input plane. Over the frequency range 500–1000 MHz and using Teflon and air, the error in the measured relative permittivity ranges between 0.04% and 0.58%, and the relative permeability ranged between 4.2% and 10%. This range is within the limits arising from inherited uncertainties of the permittivity for Teflon measurements. On the other hand, simulated results comparison with the mathematical model exhibit uncertainty ranges for both relative permittivity and permeability 0.03%–0.1%, respectively.

The results are preliminary, and the phase calibration procedure has to be refined for lossy materials where not only the phase but also the magnitude of the reflection coefficient is involved. Even so, the results show that our procedures provide a satisfactory evaluation method for complex permittivity and permeability measurements using a reflection technique.

ACKNOWLEDGMENT

This work is financially supported by TAKEOFF Seed Fund Award at University of Malta.

REFERENCES

1. Cerny, R., "Time-domain reflectometry method and its application for measuring moisture content in porous materials: A review," *Measurement*, Vol. 42, No. 3, 329–336, 2009.
2. Fellner-Feldegg, H., "Measurement of dielectrics in the time domain," *The Journal of Physical Chemistry*, Vol. 73, No. 3, 616–623, 1969.

3. Dalton, F. N. and M. Th. van Genuchten, "The time-domain reflectometry method for measuring soil water content and salinity," *Geoderma*, Vol. 38, No. 1, 237–250, 1986.
4. Nicolson, A. M. and G. F. Ross, "Measurement of the intrinsic properties of materials by time-domain techniques," *IEEE Transactions on Instrumentation and Measurement*, Vol. 19, No. 4, 377–382, 1970.
5. *Agilent 85070E Dielectric Probe Kit 200 MHz to 50 GHz. Technical Overview*, Agilent Technologies: Santa Clara, CA, USA, 2008.
6. Tan, X., J. Wu, J. Huang, M. Wu, and W. Zeng, "Design of a new TDR probe to measure water content and electrical conductivity in highly saline soils," *Journal of Soils and Sediments*, Vol. 19, No. 4, 377–382, 1970.
7. Jha, S. N., K. Narsaiah, A. L. Basediya, et al., "Measurement techniques and application of electrical properties for nondestructive quality evaluation of foods — A review," *Journal of Food Science and Technology*, Springer, 2017.
8. Andrea, C., B. De Egidio, and C. Giuseppe, *Broadband Reflectometry for Enhanced Diagnostics and Monitoring Applications*, Vol. 93, Springer, 2011.
9. Persico, R., F. Soldovieri, and R. Pierri, "Convergence properties of a quadratic approach to the inverse scattering problem," *Journal of Optical Society of America Part A*, Vol. 19, No. 12, 2424–2428, 2002.
10. Baker-Jarvis, J., M. D. Janezic, J. H. Grosvenor, Jr., and R. G. Geyer, "Transmission/reflection and short-circuit line method for measuring permittivity and permeability," *National Institute of Standards and Technology Technical Note*, 1355-R, 1993.
11. Persico, F. and R. Pieraccini, "Measurement of dielectric and magnetic properties of materials by means of a TDR probe: A preliminary theoretical investigation in the frequency domain," *Near Surface Geophysics*, Vol. 16, No. 2, 118–126, 2018.
12. Persico, R., I. Farhat, L. Farrugia, C. Sammut, and S. D'Amico, "An innovative use of TDR probes. First numerical validations with a coaxial cable," *Environmental and Engineering Geoscience*, 2018.
13. Staszek, K., et al., "Complex permittivity and permeability estimation by reflection measurements of open and short coaxial transmission line," *Microwave and Optical Technology Letters*, Vol. 56, No. 3, 727–732, 2014.